Neuro-Oncology 13(1):28–41, 2011.
doi:10.1093/neuonc/noq146
Advance Access publication November 12, 2010

Tamoxifen inhibits malignant peripheral nerve sheath tumor growth in an estrogen receptor–independent manner

Stephanie J. Byer, Jenell M. Eckert, Nicole M. Brossier, Buffie J. Clodfelder-Miller, Amy N. Turk, Andrew J. Carroll, John C. Kappes, Kurt R. Zinn, Jeevan K. Prasain, and Steven L. Carroll

Department of Pathology (S.J.B., J.M.E., N.M.B., B.J.C.-M., A.N.T., S.L.C.), Department of Cell Biology (N.M.B., S.L.C.), Department of Genetics (A.J.C.), Department of Medicine (J.C.K.), Department of Radiology (K.R.Z.), Department of Pharmacology and Toxicology (J.K.P.), Department of Neurobiology (S.L.C.) and the Comprehensive Cancer Center Mass Spectrometry Shared Facility (J.K.P.), University of Alabama at Birmingham

Few therapeutic options are available for malignant peripheral nerve sheath tumors (MPNSTs), the most common malignancy associated with neurofibromatosis type 1 (NF1). Guided by clinical observations suggesting that some NF1-associated nerve sheath tumors are hormonally responsive, we hypothesized that the selective estrogen receptor (ER) modulator tamoxifen would inhibit MPNST tumorigenesis in vitro and in vivo. To test this hypothesis, we examined tamoxifen effects on MPNST cell proliferation and survival, MPNST xenograft growth, and the mechanism by which tamoxifen impeded these processes. We found that 1–5 μM 4-hydroxy-tamoxifen induced MPNST cell death, whereas 0.01–0.1 μM 4-hydroxy-tamoxifen inhibited mitogenesis. Dermal and plexiform neurofibromas, MPNSTs, and MPNST cell lines expressed ERβ and G-protein-coupled ER-1 (GPER); MPNSTs also expressed estrogen biosynthetic enzymes. However, MPNST cells did not secrete 17β-estradiol, exogenous 17β-estradiol did not stimulate mitogenesis or rescue 4-hydroxy-tamoxifen effects on MPNST cells, and the steroidal antiestrogen ICI-182,780 did not mimic tamoxifen effects on MPNST cells. Further, ablation of ERβ and GPER had no effect on MPNST proliferation, survival, or tamoxifen sensitivity, indicating that tamoxifen acts via an ER-independent mechanism. Consistent with this hypothesis, inhibitors of calmodulin (trifluoperazine, W-7), another known tamoxifen target, recapitulated 4-hydroxy-tamoxifen effects on MPNST cells. Tamoxifen was also effective in vivo, demonstrating potent antitumor activity in mice orthotopically xenografted with human MPNST cells. We conclude that 4-hydroxy-tamoxifen inhibits MPNST cell proliferation and survival via an ER-independent mechanism. The in vivo effectiveness of tamoxifen provides a rationale for clinical trials in cases of MPNSTs.

Keywords: calcium signaling, neurofibromatosis, steroid receptors, Schwann cell, xenograft model.

Patients with neurofibromatosis type 1 (NF1) develop multiple benign peripheral nerve sheath tumors known as neurofibromas.[1] Neurofibromas, which are composed of neoplastic Schwann cells admixed with fibroblasts, perineurial cells, vascular elements, and mast cells,[2] arise within skin (dermal neurofibromas), large nerves, and nerve plexuses (plexiform neurofibromas). Although histologically similar, the clinical behavior of these neurofibroma subtypes is distinct.[2,3] Dermal neurofibromas frequently develop during puberty and pregnancy, suggesting that they are hormonally responsive, and virtually never give rise to higher grade neoplasms. In contrast, plexiform neurofibromas are typically congenital and can evolve into malignant peripheral nerve sheath tumors (MPNSTs), the most common malignancy associated with NF1.[2] Indeed, NF1 patients have an 8%–13% lifetime risk of developing MPNSTs.[4] Approximately two-thirds of the MPNSTs diagnosed annually arise in NF1 patients,[5] with the remainder occurring sporadically.[6]

Received December 27, 2009; accepted August 13, 2010.

Corresponding Author: Steven L. Carroll, MD, PhD, Department of Pathology, University of Alabama at Birmingham, 1720 Seventh Avenue South, SC930G3, Birmingham, AL 35294-0017 (scarroll@uab.edu).

Patients with MPNSTs have a grim prognosis, with 5- and 10-year survival rates of 34% and 23%, respectively.[5,7] Surgery is the primary treatment for these neoplasms.[8] However, MPNSTs aggressively invade adjacent tissues and metastasize, which often makes the complete resection impossible. In this circumstance, therapeutic options are limited. Radiotherapy helps control local disease and delays recurrence but has little effect on survival.[9] At present, there are no effective chemotherapeutic regimens for treating these sarcomas.[8] Identifying new pharmaceutical agents that inhibit the proliferation and survival of neoplastic Schwann cells is thus critically important.

The potential hormonal responsiveness of some NF1-associated peripheral nerve sheath tumors raises the question of whether estrogenic signaling promotes MPNST pathogenesis. This led us to test the hypothesis that 4-hydroxy-tamoxifen, an active metabolite of the selective estrogen receptor (ER) modulator (SERM) tamoxifen, inhibits the proliferation and survival of neoplastic Schwann cells derived from NF1-associated and sporadic MPNSTs. We found that 4-hydroxy-tamoxifen does indeed inhibit the proliferation and survival of MPNST cells at concentrations equivalent to those that have similar effects on breast carcinoma cells. MPNST cells express 2 ERs [ERβ and G-protein–coupled ER-1 (GPER)] and key estrogen biosynthetic enzymes. However, several lines of evidence indicate that MPNST proliferation, survival, and tamoxifen responsiveness are not dependent on either estradiol or ERs. In keeping with these in vitro observations, we found that tamoxifen demonstrates in vivo antitumor activity in an orthotopic xenograft model of human MPNSTs.

Materials and Methods

Human Tissues

These studies were approved by the University of Alabama–Birmingham (UAB) Institutional Review Board for Human Use. The Southern Division of the Cooperative Human Tissue Network/UAB Tumor Bank (director, William Grizzle, MD, PhD) provided non-neoplastic human sciatic nerve and surgically resected dermal neurofibromas, plexiform neurofibromas, and MPNSTs for this study.

Antibodies and Reagents

Antibodies were from the following sources: mouse anti-ERα monoclonal antibody (clone 1D5), Thermo Scientific; mouse anti-ERβ monoclonal antibody (clone 9.88), Sigma-Aldrich; rabbit anti-GPER antibody (ab12563), Abcam; rabbit antiaromatase antibody (ab18995), Abcam; rabbit antiphosphoERK antibody (#9101), Cell Signaling; mouse anti-Ki67 monoclonal antibody (#558078), BD Biosciences; and mouse anti–glyceraldehyde-3-phosphate dehydrogenase (GAPDH) monoclonal antibody (clone 6C5), Fitzgerald Antibodies and Antigens. Secondary antibodies were from Jackson Immunoresearch, Inc. and BD Biosciences.

The GPER agonist G1, 4-hydroxy-tamoxifen, W-7, GF109203X, cyclosporin A, and KN-93 were obtained from EMD Chemicals. 17β-Estradiol and trifluoperazine were purchased from Sigma. ICI-182,780 was from Tocris Bioscience.

Cell Lines

We have described the sources of the MPNST lines used in this study[10] except for S462 MPNST cells, which were kindly provided by Drs. Lan Kluwe and Victor Mautner (University Hospital Eppendorf, Hamburg, Germany). MCF-7 breast carcinoma cells were from the American Type Culture Collection. Cells were maintained in Dulbecco's modified Eagle's medium (DMEM) supplemented with 10% fetal calf serum, 10 μg/mL streptomycin, and 10 IU/mL penicillin (DMEM10).

The morphology and doubling times of all cell lines were routinely assessed; cells were also regularly tested for *Mycoplasma* infection. To rule out contamination by other nonhuman cells and monitor cell identity, MPNST lines were karyotyped and shown to carry human chromosomes, albeit with abnormal karyotypes.

DNA Synthesis Assays

Incorporation of ^{3}H-thymidine was assayed in cells maintained in Schwann cell defined medium (SCDM), using our previously described methodology.[11] Experiments were performed in triplicate, with 6 replicates per condition in each experiment. Data were analyzed using a one-way ANOVA, followed by a Tukey post-hoc test, with $P < .05$ considered statistically significant.

Cell Viability Assays

Forty thousand cells per well were plated in DMEM10 overnight and then maintained in SCDM for 16–18 hours. 4-Hydroxy-tamoxifen or vehicle (dimethyl sulfoxide [DMSO]) was then added to each well. Twenty-four hours later, cells were rinsed with Hanks' balanced salt solution (HBSS) and then incubated for 30 minutes at room temperature in 200 μL of 4 ng/mL calcein acetomethoxy (AM) in HBSS. Signals were measured using a fluorescent plate reader.

Real-time PCR Assays

Real-time quantitative PCR was performed using an ABI 7500 Real Time PCR System (Applied Biosystems, Inc.) per our previously described protocol.[12] Steroid sulfatase, aromatase, ERα, ERβ, and GPER cDNA levels were assayed using TaqMan minor groove binder (MGB) probes labeled with 6-carboxyfluorescein dye (ABI assays Hs00165853_m1, Hs00240671_m1, Hs00174860_m1, Hs00230957_m1, and Hs00173506_m1, respectively), whereas 18S ribosomal levels were

assayed in the same cDNAs using TaqMan MGB probes labeled with VIC dye (Applied Biosystems # 4319413E). Assays were performed in triplicate, and target transcript levels were normalized to the level of 18S cDNA in the same reverse transcription reaction. Controls lacking added template were performed in parallel with each primer set to verify an absence of contamination.

Immunoblot Analyses

Immunoblotting was performed as per our previously described methodology.[13] Antibody dilutions were: anti-ERα, 1:250; anti-ERβ, 1:1000; anti-GPER, 1:700; anti-aromatase, 1:350; and anti-phosphoERK, 1:500. Equivalent loading was verified by reprobing membranes with anti-GAPDH antibody (1:20 000 dilution).

Mass Spectrometric Analyses of Estrogen Levels

17β-Estradiol levels in conditioned medium were quantified as previously described with minor modifications.[14] Analyses by liquid chromatography with tandem mass spectrometry (LC-MS/MS) were performed using a model SIL-HT refrigerated Shimadzu autosampler (Shimadzu Scientific Instruments) and an API 4000 (Applied Biosystems /MDS Sciex) coupled to a 100 × 2.0 mm i.d. phenyl–hexyl column pre-equilibrated with 0.1% formic acid. The mobile phase consisted of 0.1% formic acid (solvent A) and acetonitrile containing 0.1% formic acid (solvent B). Gradients were begun at 25% solvent B, linearly increased to 100% B over 3 minutes, maintained at 100% B for 3 minutes, and then returned to 25% B. Eluents (flow rate 0.3 mL/min) were directed into the mass spectrometer, which was equipped with an atmospheric pressure chemical ionization source operated in positive ion mode. Nitrogen was used as the curtain and collision gas. Multiple reaction monitoring (MRM) with mass transition m/z 506/171 was used to perform quantification. An 8-point calibration curve (0.005–10 μM) showed a linear and reproducible curve for dansyl-E2 with a coefficient of correlation better than 0.995. The percentage of accuracy of these concentrations was in the range of 91%–114%.

RNA Interference

Target sequences were selected using the Whitehead Institute siRNA Selection Program. Short hairpin RNAs (shRNAs) under the control of the human H1 promoter and targeting ERs or a nonsense sequence not present in the human genome were cloned into pSECneo (Ambion). GenBank reference sequences, the corresponding plasmids, and targeted mRNA regions are: ERβ, NM_001437.1: pSLC583, nucleotides 663–681 and GPER, NM_001031682.1: pSLC584, nucleotides 1154–1172; pSLC616, nucleotides 2914–2934 and pSLC605, nucleotides 1304–1322. Plasmids were transfected using FuGENE 6 (Roche) and stable transfectants selected using 800 μg/mL G418.

Measurement of ERβ-induced Signal Transduction

ERβ-induced signal transduction was assessed using a Cignal ERE Reporter Assay Kit (SuperArray) as per the manufacturer's recommendations. Firefly and *Renilla* luciferase signals were measured in transfected cells using the Dual-Glo Luciferase Assay System (Promega).

Orthotopic Xenografts and Therapeutic Regimen

ST88-14 cells were transduced with a lentiviral vector comprising cytomegalovirus–luciferase–internal ribosome entry site–puromycin. Firefly luciferase expression–positive ST88-14 cells were selected with 5 μg/mL puromycin, and then expression in selected clones was verified with in vivo light-based imaging.

For orthotopic grafting, the sciatic nerve of NIH III mice was surgically exposed, and 5×10^5 cells suspended in HBSS were injected into the midportion of the nerve in a 5-μL volume. Three days postgrafting, tamoxifen citrate pellets (25 mg in a matrix releasing tamoxifen continuously for 60 days; Innovative Research of America) were implanted subcutaneously in the upper back.

One, 3, 6, and 9 days after grafting, bioluminescence imaging was performed using an IVIS-100 system (Xenogen; Calipers Life Sciences). During imaging, mice were maintained under isoflurane anesthesia at 37°C. Images were collected with the animals oriented in the same position 10 minutes after intraperitoneal injection of 2.5 mg D-luciferin. Image acquisition times were in the range of 1–30 seconds, and it was ensured that no pixels were saturated during image collection. Light emission from tumor regions (relative photons/sec) was measured using Living Image 3.0 software from Xenogen, with regions of interest maintained at a constant size. In preliminary studies, we verified that tumor size and light emission were correlated, enabling real-time imaging of therapeutic responses (data not shown).

Determination of Ki67 and TUNEL Labeling Indices

Xenografts resected from grafted mice were fixed overnight in 10% formalin. The next morning, tissues were dehydrated through graded alcohols and CitroSolv (Fisher Scientific) and then paraffin embedded. Sections 5–6 μm thick prepared from these blocks were mounted on SuperFrost Plus slides and used for Ki67 immunohistochemistry and terminal deoxynucleotidyl transferase dUTP (2′-deoxyuridine, 5′-triphosphate) nick end labeling (TUNEL).

For Ki67 immunohistochemistry, slides were deparaffinized in CitroSolv (3 incubations of 3 minutes each), followed by 2 washes in 100% ethanol (2–3 minutes per wash), a wash in 95% ethanol (2–3 minutes), a

70% ethanol wash (2–3 minutes), a 50% ethanol wash (2–3 minutes), and rinsing in running tap water for 3–5 minutes. Antigen rescue in citrate buffer was performed by heating the slides for 20 minutes in a rice cooker and then letting them cool for 20 minutes at room temperature. Endogenous peroxidase activity was killed by incubating the slides in 3% hydrogen peroxide in phosphate-buffered saline (PBS) for 10 minutes. Slides were rinsed with PBS and then incubated in blocking buffer (5% bovine serum albumin in PBS) at 37°C for 1 hour. Ki67 monoclonal antibody (1:25 dilution in blocking buffer) was applied to the sections and incubated at 37°C in a humidified chamber for 2 hours. Following 3 PBS rinses (5 min/rinse), biotinylated goat antimouse immunoglobulin-G (1:250 dilution in blocking buffer) was applied to the sections for 1 hour at 37°C. Sections were then rinsed twice with PBS, and prediluted streptavidin–horseradish peroxide (BD Biosciences cat. # 550946) was applied to the sections for 30 minutes at room temperature. Following 2 PBS rinses, signals were developed using a DAB (3,3′ diaminobenzidine) Substrate Kit as per the manufacturer's recommendations (BD Biosciences). Sections were then dehydrated through graded alcohols and CitroSolv and coverslipped with Permount.

To detect cells with nuclear DNA fragmentation, TUNEL was performed using the DeadEnd Colorimetric TUNEL System as per the manufacturer's recommendations (Promega).

To determine Ki67- and TUNEL-labeling indices, 10–15 randomly selected 20× fields/section were photographed from each of 3 or more tumor sections; sections selected for staining were separated from one another by at least 10 sections. The total number of nuclei in each field (identified by hematoxylin staining) and the total number of Ki67- or TUNEL-positive nuclei (identified by DAB deposition) in the same field were counted (range for the number of cells counted from each tumor: 3014–5203 cells). Labeling indices were then determined by dividing the number of DAB-labeled cells in each field by the total number of cells in that field. Labeling indices in control and tamoxifen-treated tumors were averaged and compared using a two-tailed *t*-test, with *P*-values $<.05$ being considered significant.

Results

4-Hydroxy-tamoxifen Inhibits the Proliferation and Survival of MPNST Cells

4-Hydroxy-tamoxifen effects were examined in 6 human MPNST cell lines derived from tumors that arose in NF1 patients (NMS-2PC, ST88-14, T265-2c, 90-8, and S462 cells) or sporadically (STS-26T cells). To assess the effects on survival, cells were challenged with 4-hydroxy-tamoxifen for 24 hours and their viability then assessed by examining the cells' ability to cleave calcein AM, a reaction that generates a quantifiable fluorescent product. We have found that the number of viable MPNST cells correlates linearly with calcein AM cleavage under these experimental conditions ($R^2 = 0.9975$). We first challenged MPNST cells with 0.01–20 μM 4-hydroxy-tamoxifen; these concentrations were selected as they inhibit the proliferation and survival of breast carcinoma cells.[15,16] 1–20 μM 4-hydroxy-tamoxifen decreased the survival of S462 cells in a concentration-dependent manner (Fig. 1A). In the other lines, however, 1 μM 4-hydroxy-tamoxifen modestly inhibited survival, whereas a 10-μM concentration of this SERM killed virtually all of the cells. We therefore examined the effect that 4-hydroxy-tamoxifen concentrations between 1 and 10 μM had on the survival of the other 5 lines. With this range of concentrations, 4-hydroxy-tamoxifen decreased the survival of all 5 cell lines in a concentration-dependent manner (Fig. 1B). In 4 of the lines (STS-26T, NMS-2PC, 90-8, and T265-2c cells), statistically significant inhibition of survival was seen with as little as 1–2 μM 4-hydroxy-tamoxifen. Maximal inhibition of survival was achieved with 5 μM 4-hydroxy-tamoxifen in all 5 lines.

Visual inspection of 4-hydroxy-tamoxifen–treated cultures suggested that this agent induced MPNST cell death quite rapidly, with morphologic alterations, including the development of cytoplasmic granularity, rounding up, and cytoplasmic blebbing evident by 2 hours posttreatment (Fig. 1C). To determine how rapidly 4-hydroxy-tamoxifen induced death, we challenged ST88-14 and STS-26T cells with 10 μM 4-hydroxy-tamoxifen and examined their ability to cleave calcein AM 30 minutes to 4 hours later (Fig. 1D). Calcein AM cleavage was significantly reduced in both lines as early as 1 hour after exposure to 4-hydroxy-tamoxifen. These cells were also unable to exclude Trypan blue, confirming that they were dead.

Micromolar concentrations of 4-hydroxy-tamoxifen trigger apoptosis in breast cancer cells,[15] whereas nanomolar concentrations inhibit their proliferation.[16] To determine whether lower concentrations of 4-hydroxy-tamoxifen might similarly inhibit MPNST mitogenesis, the 6 MPNST cell lines were challenged with 0.01–20 μM concentrations of this agent and DNA synthesis was assessed 24 hours later. We found that 0.01 and 0.1 μM 4-hydroxy-tamoxifen, which had no effect on the survival of STS-26T and ST88-14 cells, potently inhibited the proliferation of these lines (Fig. 1E). In contrast, nanomolar concentrations of 4-hydroxy-tamoxifen did not diminish mitogenesis in NMS-2PC, 90-8, T265-2c, and S462 cells. Thus, nanomolar concentrations of 4-hydroxy-tamoxifen decrease DNA synthesis in at least some MPNST cell lines.

Human Dermal Neurofibromas, Plexiform Neurofibromas, MPNSTs, and MPNST Cell Lines Express ERs

To determine whether 4-hydroxy-tamoxifen effects on MPNST cells might be ER dependent, we examined the expression of ERα, ERβ, and GPER (also known

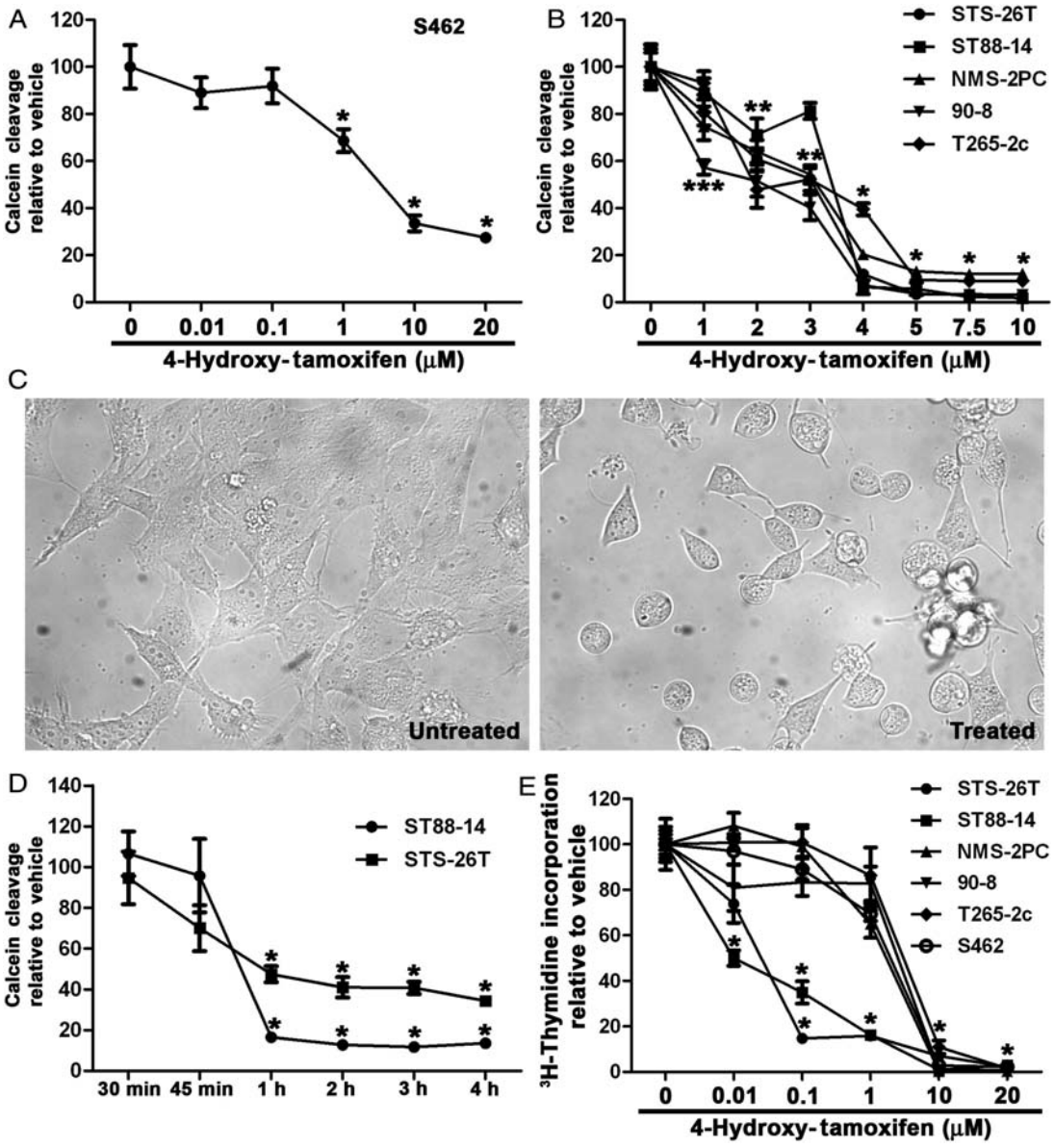

Fig. 1. 4-Hydroxy-tamoxifen inhibits the survival and proliferation of MPNST cells. (A) Calcein AM cleavage in S462 cells treated with vehicle (0) or 0.01–20 μM 4-hydroxy-tamoxifen for 24 hours. Average calcein AM cleavage and standard errors of the mean are expressed relative to cleavage in cells receiving vehicle. $*P < .05$ treatment conditions compared with vehicle-treated cells. (B) Calcein AM cleavage in STS-26T, ST88-14, NMS-2PC, 90-8, and T265-2c cells treated with vehicle (0) or 1–10 μM 4-hydroxy-tamoxifen for 24 hours. Average calcein AM cleavage and standard errors in 4-hydroxy-tamoxifen–treated cells are expressed relative to cleavage in cells receiving vehicle. $*P < .05$ for treatment conditions compared with vehicle-treated cells in all 5 lines; $**P < .05$ for all lines except ST88-14; $***P < .05$ for all lines except ST88-14 and T265-2c. (C) Photomicrographs of human ST88-14 MPNST cells after 2 hours of treatment with vehicle (left panel) or 4-hydroxy-tamoxifen (right panel). Magnification: ×40. (D) Calcein AM cleavage in ST88-14 and STS-26T cells treated with 10 μM 4-hydroxy-tamoxifen for 30 minutes to 4 hours. Calcein AM cleavage was normalized to levels assayed in parallel cultures treated with vehicle for the same time. SEMs are indicated for each condition. $*P < .05$ for comparison with untreated cells. (E) STS-26T, ST88-14, NMS-2PC, 90-8, T265-2c, and S462 cells were treated with vehicle (0) or varying concentrations of 4-hydroxy-tamoxifen and DNA synthesis measured 24 hours after initiation of treatment. Average ^{3}H-thymidine incorporation and standard errors are indicated for tamoxifen-treated cells relative to vehicle. $*P < .05$ for comparisons with control.

as GPR30) in our panel of MPNST cell lines using immunoblot analyses. ER expression in MPNST cells was compared with that in MCF-7 breast carcinoma cells, a line reported to express all 3 of these receptors.[17,18] Although ERα protein was readily detected in MCF-7 cells (Fig. 2A), it was undetectable in the 6 MPNST cell lines; consistent with this, real-time PCR assays demonstrated that ERα mRNA was expressed at exceedingly low levels in these lines (1400- to 19 000-fold lower than in MCF-7 cells;

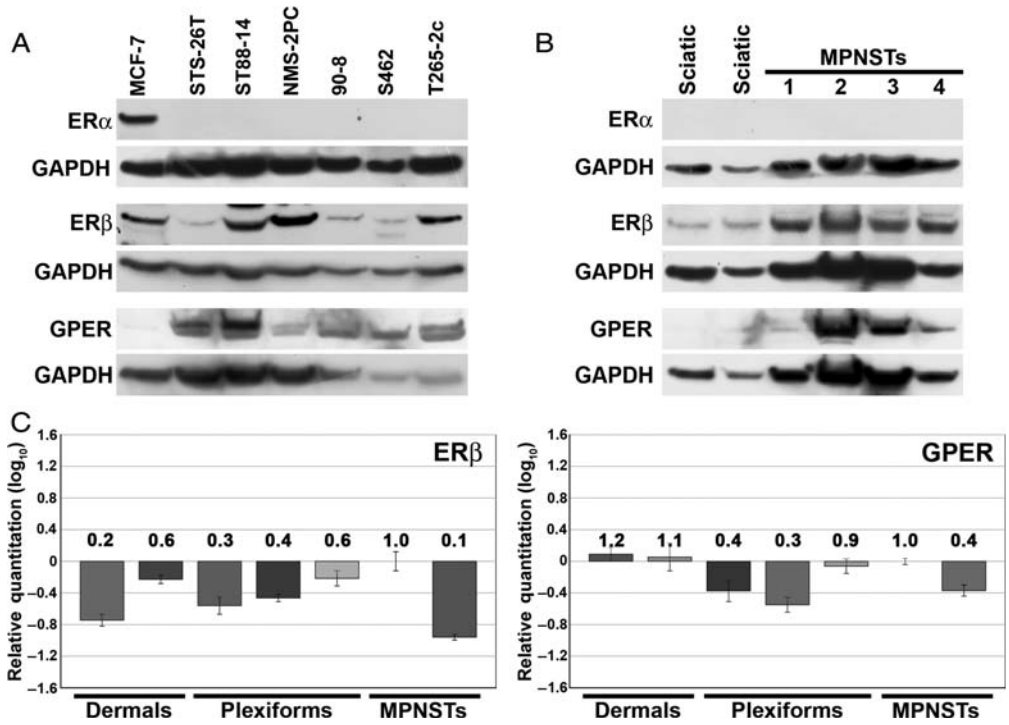

Fig. 2. MPNST cells and MPNSTs express estrogen receptors. (A) Immunoblotted lysates of MCF-7 breast carcinoma cells and 6 human MPNST cell lines (STS-26T, ST88-14, NMS-2PC, 90-8, S462, and T265-2c cells) were probed for ERα, ERβ, and GPER. Blots were reprobed for GAPDH to compare loading. (B) Immunoblotted lysates of 4 surgically resected MPNSTs and non-neoplastic sciatic nerve were probed for ERα, ERβ, and GPER. Blots were reprobed for GAPDH to compare loading. (C) Real-time quantitative PCR comparing the expression of ERβ (left panel) and GPER (right panel) mRNA in dermal neurofibromas, plexiform neurofibromas, and MPNSTs. Bars indicate relative levels of expression. Note that values are expressed on a $\log_{10}$ scale. 95% confidence intervals are indicated. Numbers above the bars indicate the fold change converted from $\log_{10}$.

Supplementary Material Fig. S1). In contrast, ERβ and GPER proteins were evident in all 6 MPNST cell lines (Fig. 2A). Levels of ERβ protein expressed in MPNST cells varied, with 3 lines having expression comparable to that in MCF-7 cells and 3 lines having somewhat lower expression. GPER expression in MPNST cells was higher than that detected in MCF-7 cells. Real-time PCR analyses showed a similar relationship between the levels of ERβ and GPER mRNAs in MPNST and MCF-7 cells (Supplementary Material, Fig. S1).

To determine whether these receptors were similarly expressed in MPNSTs in vivo, lysates of normal human sciatic nerve from 2 autopsied patients and 4 surgically resected MPNSTs were immunoblotted and probed with ER antibodies. Although ERα was undetectable in normal sciatic nerve and in all 4 tumors, both ERβ and GPER were expressed in the MPNSTs (Fig. 2B), indicating that the ERs detected in MPNST cells are similarly expressed in MPNSTs in vivo.

We next compared the expression of ERα, ERβ, and GPER in MPNSTs with that in plexiform neurofibromas, the precursor lesions from which MPNSTs often arise, and dermal neurofibromas, a class of tumors that have no malignant potential but are thought to be hormonally responsive. Real-time PCR analyses of ERα mRNA levels in 2 dermal neurofibromas and 3 plexiform neurofibromas showed that these benign tumors had exceedingly low ERα transcript levels, much as was seen in MPNSTs. In contrast, higher levels of ERβ and GPER mRNAs were detected in both dermal and plexiform neurofibromas (Fig. 2C). However, a comparison between the levels of these transcripts in neurofibromas and those detected in MPNSTs showed that although there was tumor-to-tumor variability, there were no major differences between the levels of expression of ERβ and GPER transcripts in these 3 peripheral nerve sheath tumor types.

Human MPNSTs and MPNST Cell Lines Express Estrogen Biosynthetic Enzymes

The media used in our cell survival experiments were not supplemented with 17β-estradiol. However, given the potent effects 4-hydroxy-tamoxifen demonstrated on MPNST cells, we considered the possibility that neoplastic Schwann cells in MPNSTs, such as non-neoplastic glia,[19] might make their own estrogen and thus not be dependent on exogenous hormone. As an initial test of this hypothesis, we examined the expression of transcripts encoding the rate-limiting enzymes in the 2 major estrogen biosynthetic pathways (aromatase and steroid sulfatase) in our MPNST cell lines. Aromatase and steroid sulfatase mRNA levels in MPNST cells

were compared with those in MCF-7 cells, which are known to express steroid sulfatase[20] and low levels of aromatase.[21] Aromatase transcripts were detectable in MCF-7 cells, but at levels that precluded an accurate quantitation. Higher levels of aromatase mRNA were evident in the 6 MPNST lines (Fig. 3A, left panel). Steroid sulfatase transcripts were also present in all 6 MPNST cell lines, at levels 1.5- to 4.8-fold higher than in MCF-7 cells (Fig. 3A, right panel). Immunoblot analyses confirmed the presence of aromatase protein in these MPNST lines and surgically resected MPNSTs (Supplementary Material, Fig. S2). These observations and our demonstration that ERβ and GPER are expressed by MPNST cells raised the question of whether tamoxifen might inhibit MPNST proliferation and survival by disrupting autocrine or paracrine estrogen signaling.

4-Hydroxy-tamoxifen Effects on MPNST Cells Are Not Due to Inhibition of Estrogen Action

Given their expression of estrogen biosynthetic enzymes, we next asked whether MPNST cells secrete estrogen. To answer this question, we used liquid chromatography tandem mass spectrometry to detect and quantify the levels of 17β-estradiol (E2) present in serum-free SCDM conditioned by MPNST cells for 72 hours. To enhance the sensitivity and selectivity of these assays, ethyl acetate extracts of conditioned media were reacted with dansyl chloride. Dansylation, which forms a phenyl sulfonate bond at the 3-position on the A-ring of unconjugated estrogens, has been widely used to facilitate E2 quantification in biological samples.[14,22] Full-scan MS spectrums of a 3-dansyl-E2 standard solution showed a protonated molecular ion $[M + H]^+$ at m/z 506 that, upon fragmentation in the collision cell of the tandem mass spectrometer, yielded a pronounced peak at m/z 171. Consequently, assays were performed using MRM mode with mass transition m/z 506/171 for detection and quantification of dansyl-E2. Under these conditions, the lower limit of quantification (5 nM) showed a peak with signal to noise ratio of 18 (Fig. 3B, left panel).

Quantifying E2 in unconditioned SCDM and media conditioned by MPNST (ST88-14, S462, T265-2c, and STS-26T) or control (MCF-7) cell lines, we found that dansyl-E2 was readily detected in MCF-7 conditioned medium (Fig. 3B, right panel). However, there was no evidence of dansyl-E2 in media conditioned by the 4 MPNST cell lines.

We next asked whether exogenous E2 promotes MPNST mitogenesis by challenging 4 MPNST cell lines (STS-26T, ST88-14, NMS-2PC, and 90-8 cells) for 24 hours with varying concentrations (0.1, 1, 10, or 100 nM) of E2 and examining the effect this had on ^{3}H-thymidine incorporation. E2 produced no

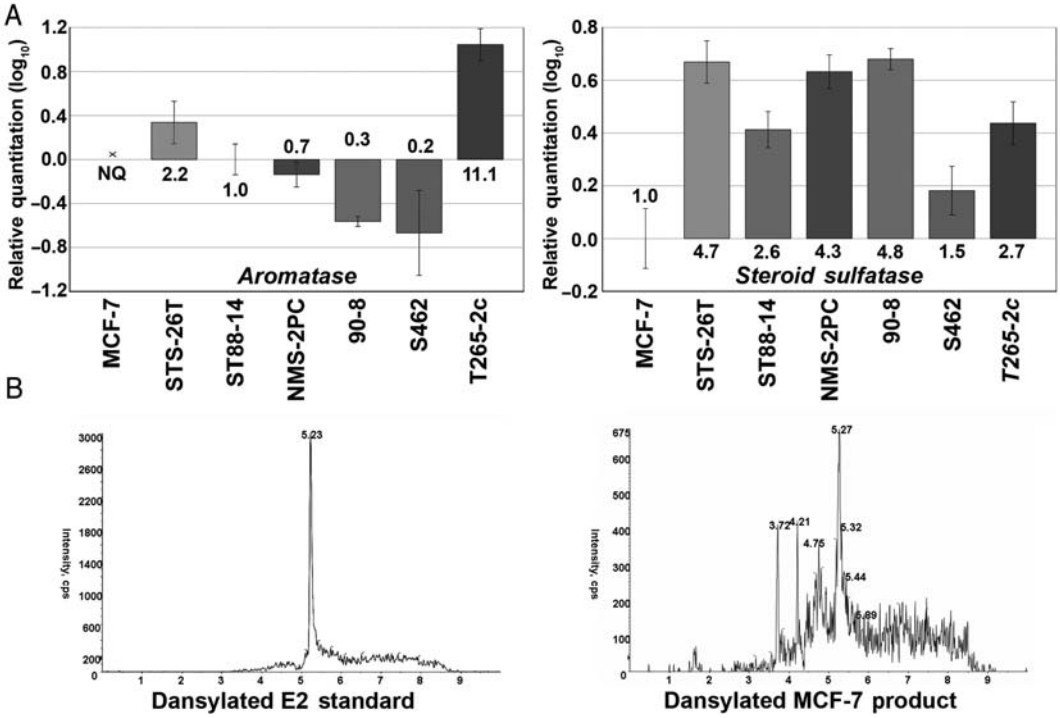

Fig. 3. (A) Real-time quantitative PCR comparing the expression of aromatase (left panel) and steroid sulfatase (right panel) mRNA in MCF-7 cells and 6 MPNST cell lines. Bars indicate relative levels of expression, with expression in ST88-14 and MCF-7 cells designated as 1 in the left and right panels, respectively. Note that values are expressed on a $\log_{10}$ scale. 95% confidence intervals are indicated. Numbers above or below the bars indicate the fold change converted from $\log_{10}$. NQ = detected, but at levels precluding accurate quantitation. (B) MRM chromatograms with mass transition m/z 506/171 for 5 nM dansylated E2 standard (left panel) and dansylated product from MCF-7 conditioned medium (right panel).

statistically significant changes in DNA synthesis in any of these 4 lines at all concentrations tested (Supplementary Material, Fig. S3A). In non-neoplastic Schwann cells, estradiol maximally stimulates proliferation when administered in combination with agents that elevate cAMP such as forskolin.[23] We therefore repeated these experiments, this time challenging ST88-14 and STS-26T cells with 0.1–100 nM E2 in combination with 5 μM forskolin. Even in the presence of forskolin, however, E2 did not enhance the MPNST cell mitogenesis (data not shown).

The failure of MPNST cells to synthesize E2 or proliferate in response to exogenous E2 suggested that tamoxifen did not act by interfering with estrogenic signaling. In support of this hypothesis, we found that 10–1000 nM E2 did not rescue STS-26T cells from death induced by 10 μM 4-hydroxy-tamoxifen (Supplementary Material, Fig. S3B) or restore the decrease in proliferation produced by 0.1 μM (100 nM) 4-hydroxy-tamoxifen (data not shown). Further, upon challenging STS-26T and ST88-14 cells with 10 and 100 nM concentrations of ICI-182,780 (IC_{50} = 0.3 nM), a steroidal antiestrogen that has pure antiestrogenic effects at these concentrations,[24] we found that this compound did not recapitulate 4-hydroxy-tamoxifen effects on MPNST cell survival (Supplementary Material, Fig. S3C). Taken together, these findings indicate that 4-hydroxy-tamoxifen does not inhibit MPNST proliferation and survival via inhibition of estrogen action.

MPNST Cell Proliferation and Survival Are Not Dependent on ERβ or GPER

In some cell types, ERs are activated by "cross-talk" with other growth factor–activated signaling pathways and can promote proliferation even in the face of estrogen withdrawal.[25] To determine whether ERβ or GPER is required for MPNST proliferation and/or survival, we transfected plasmids encoding shRNAs targeting these receptors into ST88-14 MPNST cells. As initial experiments showed no evidence of increased death in transiently transfected cultures, we generated sublines that were stably transfected with these plasmids. Immunoblot analyses confirmed that ERβ and GPER expression was markedly reduced in cells stably transfected with ER-targeting shRNAs relative to the parent line or cells transfected with a nonsense control plasmid (Fig. 4A). To verify that ERβ signaling was effectively impaired, cells were transiently transfected for 48 hours with an estrogen response element–luciferase reporter. Following a 24-h challenge with vehicle or 1–25 nM 17β-estradiol, baseline levels of luciferase activity were evident in ST88-14 cells, which increased in a concentration-dependent manner with 17β-estradiol stimulation (Fig. 4B). In contrast, neither baseline nor inducible luciferase expression was seen in cells carrying the ERβ shRNA, indicating that ERβ signaling had been abolished. To establish that GPER signaling was effectively impaired, parent ST88-14 cells and cells transfected with GPER shRNA were challenged with the GPER-specific agonist G1. This agonist induced phosphorylation of ERK 1/2 in the parent line, but not in cells expressing the GPER shRNA (Fig. 4C), verifying a loss of GPER signaling.

Despite the ablation of ERs, ^{3}H-thymidine incorporation assays indicated that DNA synthesis was neither consistently nor significantly reduced in ST88-14 sublines stably transfected with ERβ or GPER shRNAs when compared with the parent line or cells transfected with nonsense control shRNA (Fig. 4D). We conclude that ERβ and GPER signaling contribute minimally, if at all, to the proliferation and survival of these MPNST cells in vitro. Further, ablation of ERβ or GPER expression did not impede tamoxifen-induced death (Fig. 4E), indicating that tamoxifen inhibits MPNST proliferation and survival via an ER-independent mechanism.

Calmodulin Inhibitors Recapitulate 4-Hydroxy-tamoxifen Effects on MPNST Cells

Tamoxifen and its metabolites also bind directly to the calcium-binding protein calmodulin and to protein kinase C (PKC) isozymes[26] and inhibit their action.[26–29] To determine whether inhibition of calmodulin and/or PKC would recapitulate 4-hydroxy-tamoxifen effects, we challenged STS-26T and ST88-14 cells for 24 hours with inhibitors of calmodulin (trifluoperazine, W-7) or GF109203X, a broad-spectrum PKC inhibitor that targets multiple PKC isozymes (PKCα, β_I, β_{II}, γ, δ, and ε), and examined the effect this had on MPNST survival and mitogenesis. Twenty-five, 50, and 100 nM GF109203X (IC_{50} for PKC ≈ 10 nM) had no effect on the survival and proliferation of either line (Supplementary Material, Fig. S4). However, trifluoperazine inhibited the survival of STS-26T and ST88-14 cells in a concentration-dependent fashion, with statistically significant effects becoming evident at 5 μM and nearly complete inhibition achieved with 10 μM trifluoperazine (Fig. 5A, left panel). W-7 similarly impaired MPNST cell survival (Fig. 5A, right panel), with statistically significant effects on ST88-14 cells first observed with 10 μM W-7 and inhibition of STS-26T survival first seen in cells treated with a 15-μM concentration of this drug. Trifluoperazine and W-7 also produced concentration-dependent reductions in DNA synthesis in both MPNST cell lines. As with 4-hydroxy-tamoxifen, the effects of these calmodulin inhibitors on proliferation were observed at concentrations lower than those that induced cell death. Trifluoperazine 2.5-μM significantly reduced ^{3}H-thymidine incorporation in both lines (Fig. 5B, left panel), whereas 5 and 10 μM W-7 produced a significant inhibition of proliferation in ST88-14 and STS-26T cultures, respectively (Fig. 5B, right panel). To determine whether these calmodulin inhibitors, such as 4-hydroxy-tamoxifen, rapidly induced MPNST cell death, we challenged ST88-14 and STS-26T cells with 10 μM trifluoperazine

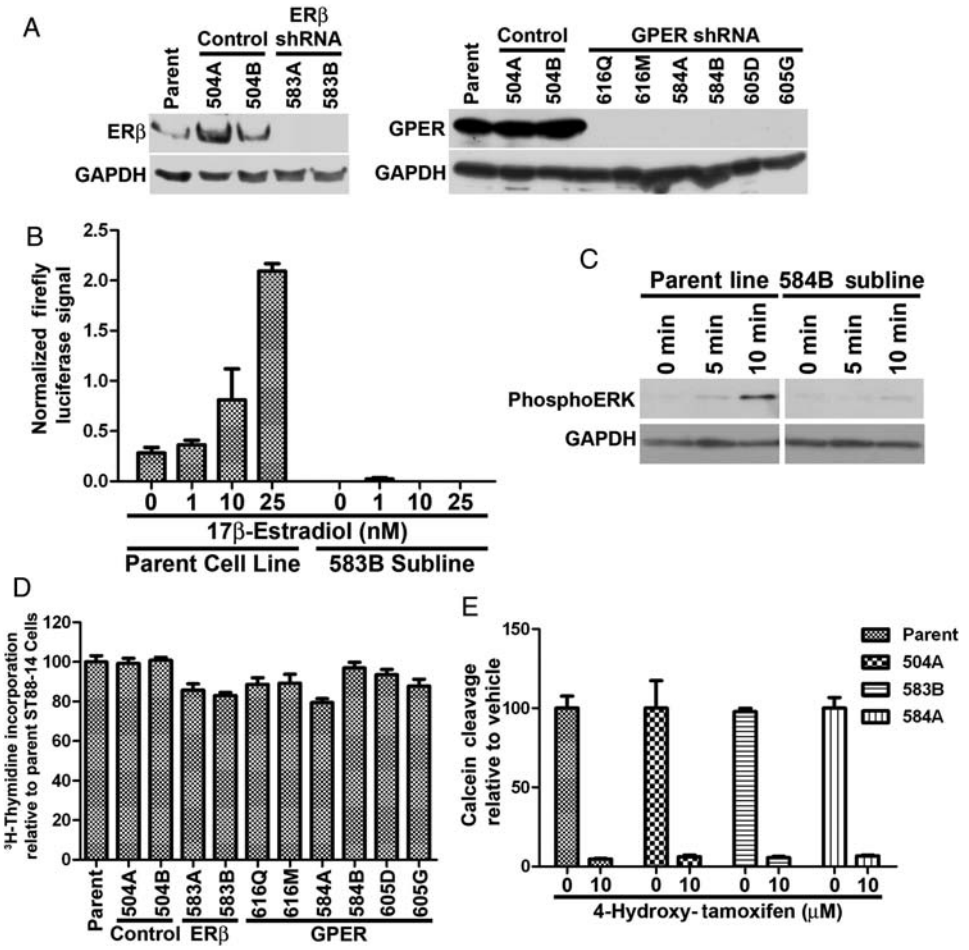

Fig. 4. MPNST proliferation, survival, and tamoxifen responsiveness is ER independent. (A) Immunoblot analyses indicate that ERβ (left panels) and GPER (right panels) expression is ablated in ST88-14 cells stably transfected with plasmids expressing shRNAs targeting mRNAs encoding these receptors, but not in the parent line or ST88-14 cells stably transfected with a plasmid expressing a nonsense control shRNA (Control). Numbers above lanes indicate the transfected shRNA plasmid, with individual sublines identified by a letter following the plasmid number. Blots were reprobed for GAPDH to verify equal loading. (B) Estrogen response element–firefly luciferase reporters were transiently transfected into ST88-14 cells or ST88-14 cells stably transfected with an ERβ shRNA (583B). 48 hours later, cells were stimulated with 0–25 nM 17β-estradiol. Firefly luciferase activity was assayed and normalized to levels of *Renilla* luciferase expressed from a cotransfected constitutively active plasmid. (C) ST88-14 cells and ST88-14 cells stably transfected with a GPER shRNA were challenged for the indicated times with the GPER-specific agonist G1. Lysates of these cultures were immunoblotted and probed for phosphorylated ERK 1/2. Blots were reprobed for GAPDH to verify equal loading. (D) Average ^{3}H-thymidine incorporation and standard errors are indicated for ST88-14 cells (Parent) and sublines transfected with a nonsense control (Control) or shRNAs targeting ERβ or GPER. Levels of ^{3}H-thymidine incorporation are normalized to levels in the parent ST88-14 line. (E) ST88-14 cells (Parent) and sublines transfected with a nonsense control (Control), ERβ shRNA (583A) or GPER shRNA (584A) were challenged with vehicle (0) or 10 μM 4-hydroxy-tamoxifen for 24 hours and their ability to cleave calcein AM was then measured. Average calcein AM cleavage and standard errors are indicated and normalized to levels in the parent ST88-14 line.

and examined their ability to cleave calcein AM 30 minutes to 4 hours later. We found that MPNST survival was reduced in both lines within the first hour of treatment (Fig. 5C).

Tamoxifen Demonstrates Antitumor Activity in an Orthotopic Xenograft Model of Human MPNSTs

To determine whether tamoxifen inhibits tumor growth in vivo, we grafted luciferase-expressing ST88-14 MPNST cells into the sciatic nerves of 16 NIH III mice. Bioluminescent imaging was performed 1 and 3 days postgrafting and verified that the grafts were established and growing. After completing imaging 3 days postgrafting (Day 0 of treatment), half of the mice were surgically implanted with tablets containing 25 mg of tamoxifen in a matrix that releases this drug continuously for 60 days. To assess tumor responses in the early stages of treatment, animals were re-imaged 3 and 6 days after implantation of the tamoxifen tablets. As illustrated by the representative images shown in Fig. 6A, bioluminescent signals from the orthotopic

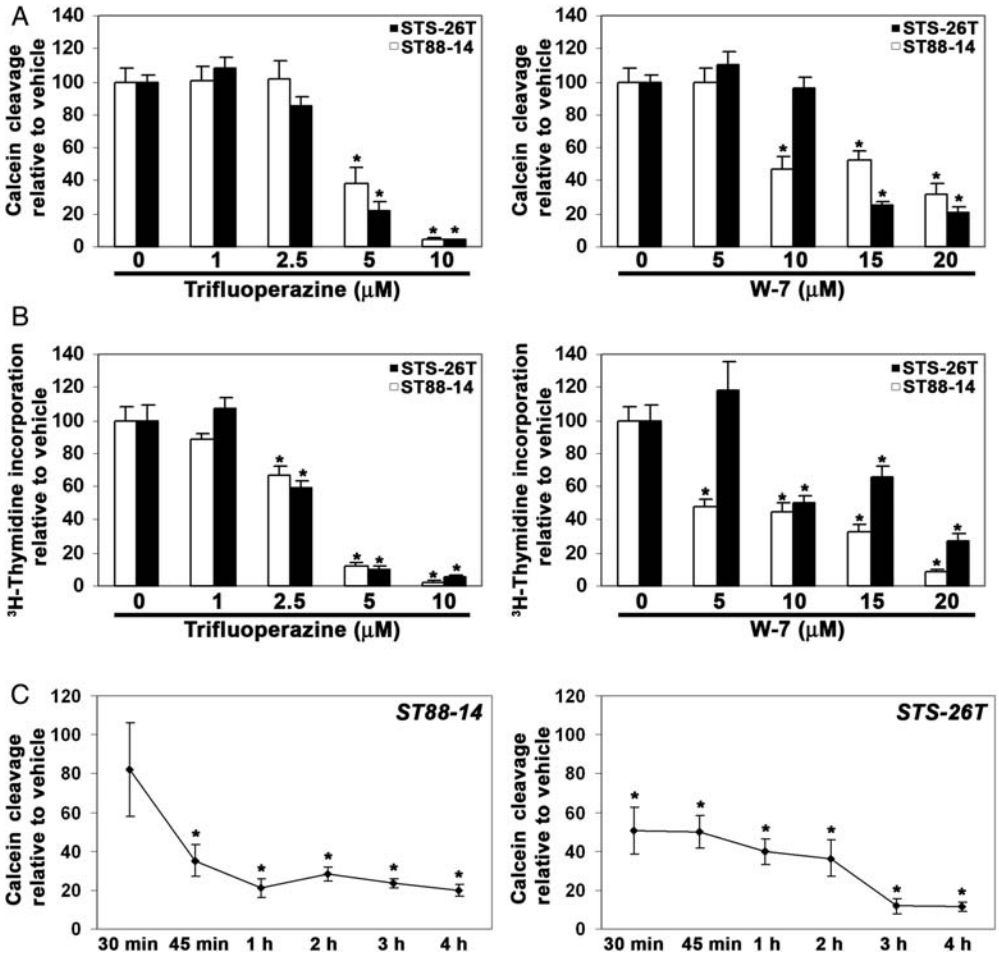

Fig. 5. Calmodulin inhibitors mimic 4-hydroxy-tamoxifen effects on MPNST cell survival and proliferation. (A) ST88-14 (white bars) and STS-26T (black bars) cells were treated with the indicated concentrations of the calmodulin inhibitors trifluoperazine (left panel) or W-7 (right panel) and calcein AM cleavage was measured 24 hours later. (B) ST88-14 (white bars) and STS-26T (black bars) cells were treated with the indicated concentrations of the calmodulin inhibitors trifluoperazine (left panel) or W-7 (right panel) and ^{3}H-thymidine incorporation was measured 24 hours later. In (A) and (B), bars indicate average measurements in inhibitor-treated cells relative to cells receiving vehicle (0). SEMs are indicated for each condition. (C) Calcein AM cleavage in ST88-14 (left panel) and STS-26T (right panel) MPNST cells 30 minutes to 4 hours after the initiation of treatment with 10 μM trifluoperazine. Calcein AM cleavage was normalized to the levels of calcein AM cleavage assayed in parallel cultures treated with vehicle for the same time. SEMs are indicated for each condition. For (A), (B), and (C), asterisks indicate a *P*-value of $<.05$ for comparisons with vehicle-treated cells.

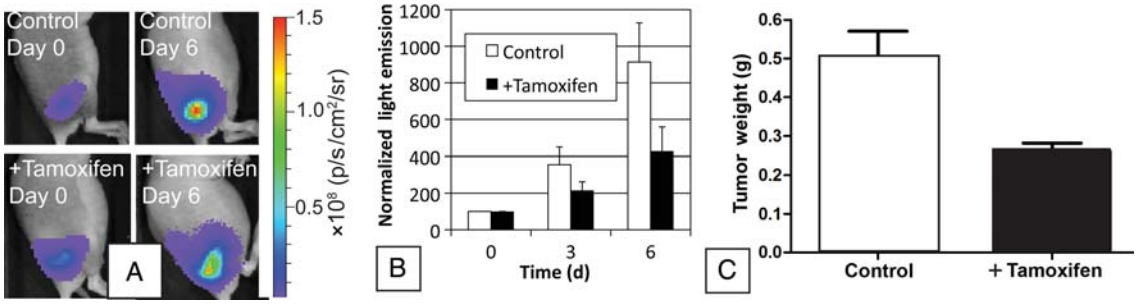

Fig. 6. Representative bioluminescence images of mice with luciferase-positive ST88-14 orthotopic xenografts (A), together with tumor region of interest data (mean ± standard error) over time for all mice (B), and tumor weights at termination (C). The tamoxifen pellet was implanted after imaging on Day 0. For Fig. 6B, the region of interest data for each mouse were normalized to its individual bioluminescence signal on Day 0 (×100%), prior to initiation of treatment.

xenografts were lower in mice treated with tamoxifen. Quantification of tumor region of interest data from the 8 tamoxifen-treated and 8 control mice confirmed that the tamoxifen-treated group showed an approximately 2-fold reduction in tumor growth in the first week of treatment (Fig. 6B). Due to rapid growth of the grafts in the control group, the experiment was terminated 18 days after the initiation of therapy and the grafts were collected. A comparison of the weights of these grafts showed that the grafts from the tamoxifen-treated mice weighed half as much as those of the control group (Fig. 6C), consistent with the results of the bioluminescence imaging.

Pathologic examination of the grafts from the control group (Fig. 7A, left panel) demonstrated the presence of spindled tumor cells with brisk mitotic activity; the morphology of these cells was consistent with that of cultured ST88-14 cells. These same cells were present in the grafts from tamoxifen-treated mice. However, extensive areas of geographic necrosis and numerous apoptotic bodies were also evident in these latter grafts, and individual tumor cells demonstrated

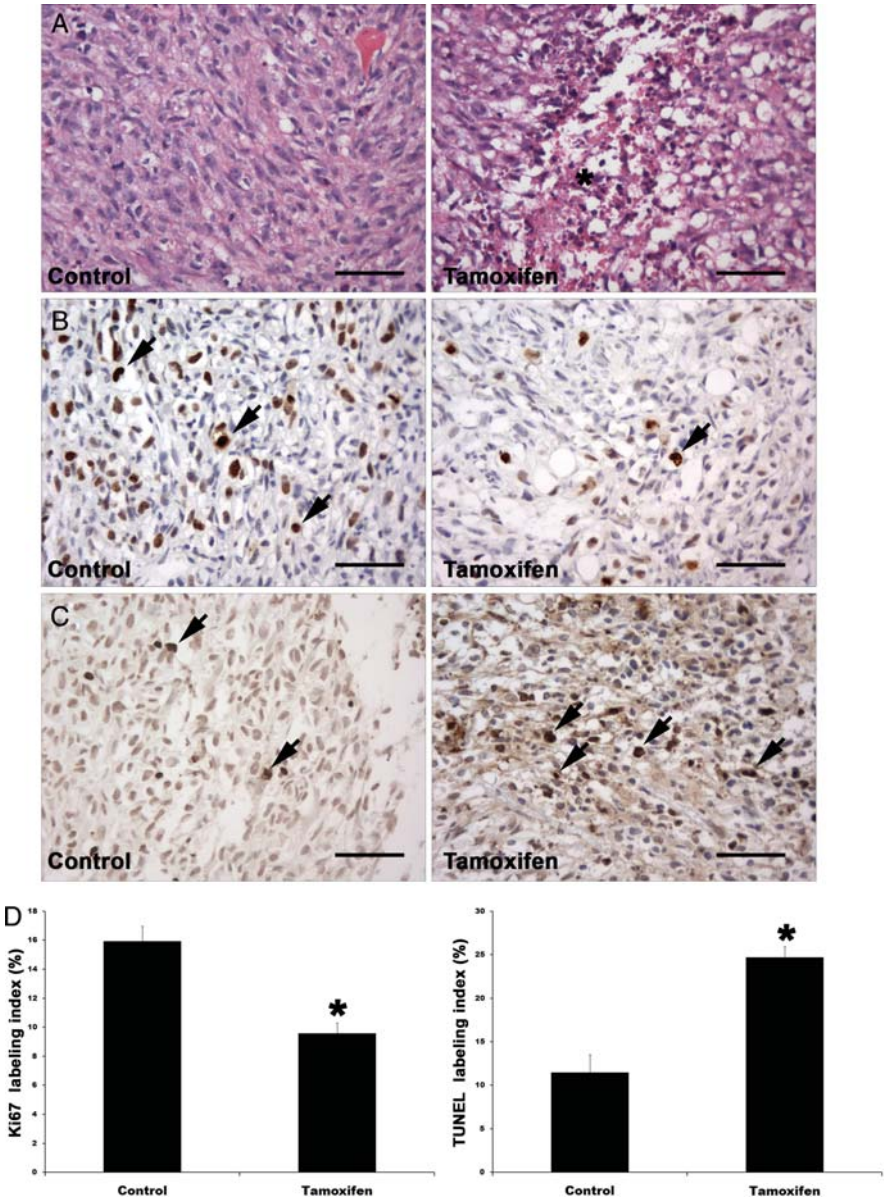

Fig. 7. Tamoxifen inhibits MPNST proliferation and survival in vivo. (A) Representative hematoxylin and eosin–stained sections from control (left panel) and tamoxifen-treated (right panel) grafts. The asterisk in the right panel indicates an area of geographic necrosis. (B) Representative images of Ki67 labeling in control (left panel) and tamoxifen-treated (right panel) grafts. Arrows indicate some of the Ki67-immunoreactive tumor cell nuclei in these sections. (C) Representative images of TUNEL staining in control (left panel) and tamoxifen-treated (right panel) grafts. Arrows indicate some of the TUNEL-positive cells in these sections. Bars in (A), (B), and (C) = 200 μm. (D) Average Ki67 (left panel) and TUNEL (right panel) labeling indices in 4 control and 4 tamoxifen-treated grafts. *$P \ll .05$.

prominent cytoplasmic vacuolation (Fig. 7A, right panel). To more rigorously establish whether tamoxifen treatment inhibited the proliferation and survival of the grafted MPNST cells, Ki67 immunohistochemistry and TUNEL were performed on sections from 4 control grafts and 4 tamoxifen-treated grafts. Initial inspection of these stained sections via light microscopy demonstrated that the number of Ki67-labeled cells was reduced in tamoxifen-treated grafts (Fig. 7B) and that there was an increase in the number of TUNEL-positive cells in these same grafts (Fig. 7C). Determination of the Ki67-labeling indices in these tumors (Fig. 7D, left panel) demonstrated that there was indeed a striking reduction in the number of Ki67-positive MPNST cells in tamoxifen-treated grafts (16% in controls vs 9.6% in tamoxifen-treated; $P < .05$). The increase in the TUNEL index in the tamoxifen-treated grafts (Fig. 7D, right panel) was even more striking (11.5% in controls vs 24.7% in tamoxifen-treated; $P < .05$). We conclude that tamoxifen also inhibits MPNST cell proliferation and survival in vivo.

Discussion

In humans, tamoxifen is rapidly converted to active metabolites including 4-hydroxy-tamoxifen and *N*-desmethyl-tamoxifen.[30,31] We found that one of these metabolites, 4-hydroxy-tamoxifen, inhibited the proliferation and survival of MPNST cells. However, while MPNST cells and MPNSTs expressed ERs and estrogen biosynthetic enzymes, MPNST cells did not secrete detectable levels of 17β-estradiol and exogenous 17β-estradiol did not stimulate MPNST cell mitogenesis or rescue 4-hydroxy-tamoxifen–mediated inhibition of MPNST cell survival and proliferation. Further, the pure antiestrogen ICI-182,780 did not mimic 4-hydroxy-tamoxifen effects on these cells, and ablation of ERβ and GPER had no effect on MPNST mitogenesis, survival, or tamoxifen sensitivity. In contrast, calmodulin inhibitors recapitulated 4-hydroxy-tamoxifen effects on MPNST cells. We conclude that 4-hydroxy-tamoxifen inhibits the proliferation and survival of MPNST cells via an ER-independent mechanism. Our observation that tamoxifen has potent antitumor activity in an orthotopic xenograft model of human MPNSTs also has important therapeutic implications.

4-Hydroxy-tamoxifen inhibited the survival of MPNST cells at low micromolar concentrations and impeded their proliferation at high nanomolar concentrations. Extensive experience with tamoxifen-sensitive breast carcinomas indicates that these concentrations of 4-hydroxy-tamoxifen are relevant in vivo. Tamoxifen has been the single agent of choice for treating ER-positive breast cancers since the early 1970s because it is effective and well tolerated and lacks severe toxicity.[16] As in MPNST cells, low micromolar concentrations of 4-hydroxy-tamoxifen inhibit the survival of breast carcinoma cells, and high nanomolar concentrations impede their proliferation.[15,16] Steady-state plasma concentrations of up to 1 μM tamoxifen are readily achieved,[32] and this agent accumulates to even higher levels (0.7–14 μM) in breast carcinomas.[25] As tamoxifen effectively penetrates the nervous system,[33,34] these observations suggest that therapeutically effective levels of tamoxifen can be delivered to MPNSTs in vivo. Consistent with this notion, we have shown that tamoxifen has potent antitumor effects in an orthotopic xenograft model of human MPNSTs. Clinical evidence also indicates that tamoxifen is unlikely to promote the death of non-neoplastic Schwann cells, as peripheral neuropathies are exceedingly rare in patients receiving tamoxifen.[35,36]

Fishbein et al. reported that tamoxifen did not inhibit proliferation in 2 MPNST cell lines and that this agent induced a slight increase in apoptosis in only 1 of these lines.[37] However, these authors examined only the effects of 1 μM tamoxifen as opposed to the range of 4-hydroxy-tamoxifen concentrations used in our studies. We have found that the concentration of 4-hydroxy-tamoxifen inducing death varies among MPNST cell lines, with some lines demonstrating impaired survival with 1 μM 4-hydroxy-tamoxifen and higher concentrations being required to induce death in other lines. Similar line-to-line variability was evident when examining 4-hydroxy-tamoxifen effects on DNA synthesis. At present, it is not clear why MPNST cell lines differ in their relative sensitivity to 4-hydroxy-tamoxifen. Answering this question will be important, however, as it will facilitate the identification of MPNSTs most likely to respond to tamoxifen therapy.

Our findings indicate that 4-hydroxy-tamoxifen inhibits MPNST cell survival and proliferation via an ER-independent mechanism. This raises the question of what role estrogen signaling plays in neoplastic Schwann cells. Non-neoplastic Schwann cells express ERs,[19,23,38] and estrogen administered in combination with forskolin stimulates their proliferation.[23] Nonetheless, 17β-estradiol alone or in combination with forskolin had no effect on MPNST mitogenesis, indicating that the estrogenic responses of neoplastic Schwann cells differ from those of non-neoplastic Schwann cells. However, our data clearly indicate that MPNST cell ERs are functional, and consequently we cannot rule out the possibility that estrogen promotes MPNST mitogenesis in an in vivo environment where other, as yet unidentified, factors that might cooperate with estrogenic signaling are present. The estrogen driving proliferation in vivo could be derived from circulating estrogens or via intratumoral conversion of circulating precursors. Consistent with this hypothesis, the proliferation of orthotopically grafted MPNST cells is diminished in ovariectomized immunodeficient mice and this decreased proliferation can be rescued with exogenous estrogen.[39] Alternatively, estrogens may regulate other functions that we have not yet examined, such as tumor cell invasion. If either of these hypotheses is correct, tamoxifen will have ER-dependent effects on MPNST growth in vivo that were not evident in our in vitro studies.

Our demonstration that the calmodulin inhibitors trifluoperazine and W-7 recapitulate 4-hydroxy-tamoxifen effects on MPNST proliferation and survival are consistent with the hypothesis that tamoxifen effects on these cells occur via an ER-independent mechanism and that

this mechanism involves inhibition of calmodulin signaling. This is also consistent with preliminary studies in which we have found that 2 calmodulin-regulated enzymes, calcineurin and CaMK, promote MPNST mitogenesis (Supplementary Material, Fig. S5). Relatively little is known regarding the role calcium signaling plays in the proliferation and survival of MPNST cells. However, it has been shown that MPNST cells stimulated with platelet-derived growth factor show an exaggerated increase in intracellular calcium and enhanced activation of CaMKII compared with non-neoplastic Schwann cells.[40] These observations, considered together with our demonstration that calmodulin inhibitors potently inhibit MPNST cell proliferation and survival, are consistent with the hypothesis that aberrant calcium signaling is essential for MPNST tumorigenesis and suggest that agents such as trifluoperazine may also be useful for the treatment of these sarcomas.

Having said that, however, we must caution that we cannot yet definitively conclude that calmodulin inhibition is the mechanism by which tamoxifen impedes the proliferation and survival of MPNST cells. Indeed, tamoxifen has been found to inhibit the survival of other tumor cell types via diverse ER-independent mechanisms, including modulation of the action of TGFβ and c-myc, activation of JNK signaling, enhanced oxidative stress, increased ceramide generation, and alterations in mitochondrial permeability transition.[16] It will be of great interest to determine whether tamoxifen acts in MPNST cells via calmodulin inhibition, other ER-independent mechanisms, or a combination of both.

In summary, our findings indicate that 4-hydroxy-tamoxifen inhibits MPNST proliferation and survival in vitro via an ER-independent mechanism. The concentrations of 4-hydroxy-tamoxifen producing these effects are readily achieved in vivo; this is inconsistent with our demonstration that tamoxifen has potent antitumor effects in an orthotopic xenograft model of human MPNSTs. Given the extensive clinical experience with tamoxifen in breast cancer patients, the fact that it is well tolerated, tamoxifen's relative lack of toxicity, and an absence of untoward effects of tamoxifen in the normal peripheral nervous system, tamoxifen is a strong candidate agent for the treatment of NF1-associated and sporadic MPNSTs. Delineating the signaling pathways affected in MPNSTs treated with tamoxifen in vivo is also likely to point to new means of treating these aggressive sarcomas, thereby expanding our currently limited therapeutic repertoire.

Supplementary Material

Supplementary material is available at *Neuro-Oncology Journal* online.

Conflict of interest statement. None declared.

Funding

This work was supported by the National Institute of Neurological Diseases and Stroke (R01 NS048353 to S.L.C.), the National Cancer Institute (R01 CA122804 to S.L.C. and CA13148-35 to K.R.Z.), and the Department of Defense (W81XWH-09-1-0086 to S.L.C.). Funds for the operation of the UAB Comprehensive Cancer Center Mass Spectrometry Shared Facility and the Small Animal Imaging Shared Facility were provided by an NCI Core Support grant (P30 CA13148-35; E. Partridge, P.I.). Support for the Genetically Defined Microbe and Expression Core of the UAB Mucosal HIV and Immunology Center, which performed the lentiviral transduction of ST88-14 cells, was provided by grant R24 DK64400.

Acknowledgments

We thank Kevin A. Roth, MD, PhD, (Department of Pathology, UAB) for helpful comments on this manuscript. We also thank the Alabama Neuroscience Blueprint Core Center (P30 NS57098) and the UAB Neuroscience Core Center (P30 NS47466) for technical assistance. The content is solely the responsibility of the authors and does not necessarily represent the official views of the National Institutes of Health or the Department of Defense.

References

1. Gutmann DH. The neurofibromatoses: when less is more. *Hum Mol Genet.* 2001;10:747–755.
2. Carroll SL, Stonecypher MS. Tumor suppressor mutations and growth factor signaling in the pathogenesis of NF1-associated peripheral nerve sheath tumors. I. The role of tumor suppressor mutations. *J Neuropath Exp Neurol.* 2004;63:1115–1123.
3. Carroll SL, Stonecypher MS. Tumor suppressor mutations and growth factor signaling in the pathogenesis of NF1-associated peripheral nerve sheath tumors. II. The role of dysregulated growth factor signaling. *J Neuropath Exp Neurol.* 2005;64:1–9.
4. Evans DGR, Baser ME, McGaughran J, Sharif S, Howard E, Moran A. Malignant peripheral nerve sheath tumors in neurofibromatosis 1. *J Med Genet.* 2002;39:311–314.
5. Woodruff JM, Kourea HP, Louis DN, Scheithauer BW. Malignant peripheral nerve sheath tumour (MPNST). In: Kleihues P and Cavenee WK, eds. *Pathology and Genetics of Tumours of the Nervous System*. 1st ed. Lyon: IARC Press; 2000:172–174.
6. Lewis JJ, Brennan MF. Soft tissue sarcomas. *Curr Probl Surg.* 1996;33:817–872.
7. Ducatman BS, Scheithauer BW, Piepgras DG, Reiman HM, Ilstrup DM. Malignant peripheral nerve sheath tumors. A clinicopathologic study of 120 cases. *Cancer* 1986;57:2006–2021.
8. Ferner RE, Gutmann DH. International consensus statement on malignant peripheral nerve sheath tumours in neurofibromatosis 1. *Cancer Res.* 2002;62:1573–1577.

9. Ferner RE, O'Doherty MJ. Neurofibroma and schwannoma. *Curr Opin Neurol.* 2002;15:679–684.
10. Stonecypher MS, Byer SJ, Carroll SL. Activation of the neuregulin-1/erbB signaling pathway promotes the proliferation of neoplastic Schwann cells in human malignant peripheral nerve sheath tumors. *Oncogene.* 2005;24:5589–5605.
11. Frohnert PW, Stonecypher MS, Carroll SL. Lysophosphatidic acid promotes the proliferation of adult Schwann cells isolated from axotomized sciatic nerve. *J Neuropath Exp Neurol.* 2003;62:520–529.
12. Stonecypher MS, Chaudhury AR, Byer SJ, Carroll SL. Neuregulin growth factors and their erbB receptors form a potential signaling network for schwannoma tumorigenesis. *J Neuropath Exp Neurol.* 2006; 65:162–175.
13. Carroll SL, Miller ML, Frohnert PW, Kim SS, Corbett JA. Expression of neuregulins and their putative receptors, ErbB2 and ErbB3, is induced during Wallerian degeneration. *J Neurosci.* 1997;17:1642–1659.
14. Nelson RE, Grebe SK, Okane DJ, Singh RJ. Liquid chromatography-tandem mass spectrometry assay for simultaneous measurement of estradiol and estrone in human plasma. *Clin Chem.* 2004;50:373–384.
15. Perry RR, Kang Y, Greaves B. Effects of tamoxifen on growth and apoptosis of estrogen-dependent and -independent human breast cancer cells. *Ann Surg Oncol.* 1995;2:238–245.
16. Mandlekar S, Kong ANT. Mechanisms of tamoxifen-induced apoptosis. *Apoptosis* 2001;6:469–477.
17. Lee YR, Park J, Yu HN, Kim JS, Youn HJ, Jung SH. Up-regulation of PI3K/Akt signaling by 17beta-estradiol through activation of estrogen receptor-alpha, but not estrogen receptor-beta, and stimulates cell growth in breast cancer cells. *Biochem Biophys Res Comm.* 2005;336:1221–1226.
18. Revankar CM, Cimino DF, Sklar LA, Arterburn JB, Prossnitz ER. A transmembrane intracellular estrogen receptor mediates rapid cell signaling. *Science.* 2005;307:1625–1630.
19. Jung-Testas I, Baulieu EE. Steroid hormone receptors and steroid action in rat glial cells of the central and peripheral nervous system. *J Steroid Biochem Mol Biol.* 1998;65:243–251.
20. Walter G, Liebl R, von Angerer E. 2-Phenylindole sulfamates: inhibitors of steroid sulfatase with antiproliferative activity in MCF-7 breast cancer cells. *J Steroid Biochem Mol Biol.* 2004;88:409–420.
21. Kitawaki J, Fukuoka M, Yamamoto T, Honjo H, Okada H. Contribution of aromatase to the deoxyribonucleic acid synthesis of MCF-7 human breast cancer cells and its suppression by aromatase inhibitors. *J Steroid Biochem Mol Biol.* 1992;43:267–277.
22. Xia YQ, Chang SW, Patel S, Bakhtiar R, Karanam B, Evans DC. Trace level quantification of deuterated 17beta-estradiol and estrone in ovariectomized mouse plasma and brain using liquid chroatography/tandem mass spectrometry following dansylation reaction. *Rapid Commun Mass Spectrom.* 2004;18:1621–1628.
23. Jung-Testas I, Schumacher M, Bugnard H, Baulieu EE. Stimulation of rat Schwann cell proliferation by estradiol: synergism between the estrogen and cAMP. *Brain Res Dev Brain Res.* 1993;72:282–290.
24. Howell A, Osborne CK, Morris C, Wakeling AE. ICI 182,780 (Faslodex): development of a novel, "pure" antiestrogen. *Cancer.* 2000;89:817–825.
25. Clarke R, Leonessa F, Welch JN, Skaar TC. Cellular and molecular pharmacology of antiestrogen action and resistance. *Pharmacol Rev.* 2001;53:25–71.
26. O'Brian CA, Ioannides CG, Ward NE, Liskamp RE. Inhibition of protein kinase C and calmodulin by the geometric isomers *cis*- and *trans*-tamoxifen. *Biopolymers.* 1990;29:97–104.
27. Gulino A, Barrera G, Vacca A, et al. Calmodulin antagonism and growth-inhibiting activity of triphenylethylene antiestrogens in MCF-7 human breast cancer cells. *Cancer Res.* 1986;46:6274–6278.
28. O'Brian CA, Housey GM, Weinstein IB. Specific and direct binding of protein kinase C to an immobilized tamoxifen analogue. *Cancer Res.* 1988;48:3626–3629.
29. Cheng AL, Chuang SE, Fine RL, et al. Inhibition of the membrane translocation and activation of protein kinase C, and potentiation of doxorubicin-induced apoptosis of hepatocellular carcinoma cells by tamoxifen. *Biochem Pharmacol.* 1998;55:523–531.
30. Lien EA, Solheim E, Ueland PM. Distribution of tamoxifen and its metabolites in rat and human tissues during steady-state treatment. *Cancer Res.* 1991;51:4837–4844.
31. Lim CK, Yuan ZK, Lamb JH, White IN, De Matteis F, Smith LL. A comparative study of tamoxifen metabolism in female rat, mouse and human liver microsomes. *Carcinogenesis.* 1994;15:589–593.
32. MacCallum J, Cummings J, Dixon JM, Miller WR. Concentrations of tamoxifen and its major metabolites in hormone responsive and resistant breast tumours. *Br J Cancer.* 2000;82:1629–1635.
33. Zhou W, Koldzic-Zivanovic N, Clarke CH, et al. Selective estrogen receptor modulator effects in the rat brain. *Neuroendocrinology.* 2002;75:24–33.
34. Kimelberg HK, Jin Y, Charniga C, Feustel PJ. Neuroprotective activity of tamoxifen in permanent focal ischemia. *J Neurosurg.* 2003; 99:138–142.
35. Bigler LR, Tate Thigpen J, Blessing JA, Fiorica J, Monk BJ, Gynecologic Oncology Group. Evaluation of tamoxifen in persistent or recurrent nonsquamous cell carcinoma of the cervix: a Gynecologic Oncology Group study. *Int J Gynecol Cancer.* 2004;14:871–287.
36. The Arimidex, Tamoxifen, Alone or in Combination Trialists' Group, Buzdar AU, et al. Comprehensive side-effect profile of anastrozole and tamoxifen as adjuvant treatment for early-stage breast cancer: long-term safety analysis of the ATAC trial. *Lancet Oncol.* 2007;7:633–643.
37. Fishbein L, Zhang X, Fisher LB, et al. In vitro studies of steroid hormones in neurofibromatosis 1 tumors an Schwann cells. *Mol Carcinog.* 2007;46:512–523.
38. Jung-Testas I, Do Thi A, Koenig H, et al. Progesterone as a neurosteroid: synthesis and actions in rat glial cells. *J Steroid Biochem Mol Biol.* 1999;69:97–107.
39. Perrin GQ, Li H, Fishbein L, et al. An orthotopic xenograft model of intraneural NF1 MPNST suggests a potential associaation between steroid hormones and tumor cell proliferation. *Lab Invest.* 2007;87:1092–1102.
40. Dang I, DeVries GH. Schwann cell lines derived from malignant peripheral nerve sheath tumors respond abnormally to platelet-derived growth factor BB. *J Neurosci Res.* 2005;79:318–328.